IJAREEIE

e-ISSN: 2278-8875
p-ISSN: 2320-3765

International Journal of Advanced Research in Electrical, Electronics and Instrumentation Engineering

Volume 10, Issue 8, August 2021

ISSN INTERNATIONAL STANDARD SERIAL NUMBER INDIA

Impact Factor: 7.282

| e-ISSN: 2278 – 8875, p-ISSN: 2320 – 3765| www.ijareeie.com | Impact Factor: 7.282|

|| Volume 10, Issue 8, August 2021 ||

| DOI:10.15662/IJAREEIE.2021.1008044 |

Design and Comparison of Classical and Improved P&O Method for PV-Wind-Battery based Grid Connected Generation System

Ramkrishna V. Kadam[1], CH.Mallareddy[2]

PG Student [M. Tech Electrical], Dept. of EE, FTC's College of Engineering and Research, Sangola, Maharashtra, India[1]

Assistant Professor, Dept. of EE, FTC's College of Engineering and Research, Sangola, Maharashtra, India[2]

ABSTRACT: In this paper, the design of a conventional P&O method and improved P&O method with sliding mode control (SMC), and active power control (APC) with anti-windup PI controller (AWPI) are investigated to get the high level of performance and stable operation of a wind-PV-battery based hybrid standalone power generation system (HSPGS). The modified MPPT technique requires a reduced no of sensors. To get the optimized trajectory of the system under variable operating conditions, the SMC approach with a boundary layer is used. The several advantages of the improved P&O method over the conventional P&O method are highlighted through the results of system simulation. Furthermore, detailed Modeling and stability analysis are discussed. The effectiveness of HSPGS with various control strategies are validated by simulation and conclusion made from obtained test results.

KEYWORDS:HSPGS – Hybrid standalone power generation system, SPVA – Solar photovoltaic array, WT – Wind Turbine SMC – Sliding Mode Control, AWPI – Anti-windup Proportional and integral controller, P&O – Perturbation and Observation method, MPPT – Maximum power point tracking, APC – Active power control, PMBLDCG – Permanent magnet brushless DC generator.

I.INTRODUCTION

Day by the day energy demand of the world is increasing due to industrialization, urbanization, transportation, and an increase in population. Still, now, major electricity demand is supplied from conventional fossil fuel-based power generation stations. The uneven distribution of fossil fuels, their limited availability, high price, and environmental factors made us move towards a renewable generation system. Many remote locations used DG set for their electricity needs, instead of that we can now implement Solar and wind energy sources with many advantages such as zero pollution, Free and abundant availability, etc… Hybrid power solutions are becoming more popular in the renewable energy sector. But it requires improvement especially in efficiency and power quality. In [1-2] The application of hybrid power solutions with microgrid and the power quality issues are discussed.

Various MPPT techniques are discussed in [3-5] These methods are: Constant voltage method, Open circuit voltage method, short-circuit current method, Perturb and Observe method, Incremental Conductance method, Temperature Parametric method, Slide control method. The P&O method is easy as compared to the above-mentioned methods. The only disadvantage of this technique is the issues of power quality due to continuous oscillations occurs around the MPP. Also, the system may take time to track MPP in case of sudden weather changes. Many other techniques are discussed in [6-8] with some modification to the conventional P&O method but, still, there is the scope of improvement in Modeling and stability analysis. Some of these techniques are complex and slow dynamics which requires large run time.

The SMC based MPPT methods are discussed in [9-11] This technique helps to achieve high performance during weather changes and for fast-tracking. However, in the above references, these methods are applied for simple systems with a reduced number of power converters. The chattering phenomenon is completely neglected which may arise due to high switching frequency with an increased number of power converters.

Active power control in HSPGS is done by controlling the DC-AC interfacing inverter using suitable control strategies like adaptive voltage control [12], fuzzy adaptive voltage control [13], improved droop control strategy [14-18]. For all the above-mentioned control strategies, the classical PI controller with inner and outer loops are used with

| e-ISSN: 2278 – 8875, p-ISSN: 2320 – 3765| www.ijareeie.com | Impact Factor: 7.282|

|| Volume 10, Issue 8, August 2021 ||

| DOI:10.15662/IJAREEIE.2021.1008044 |

consideration of saturation limit. However, once the system exceeds its physical limits, the above techniques are not enough to prevent wind up and the feedback loop breaks then, the system runs as an open loop.

An improved P&O based SMC with boundary layer is proposed in this paper to achieve improved performance in a manner of stable operation and less chattering phenomenon. APC with a reduced number of sensors is implemented for voltage regulation at Point of Common Coupling (PCC). Anti-windup (AWPI) voltage controller with optimal gain design is proposed to avoid saturation and voltage overshoot during transitions.

II.SYSTEM MODEL AND ASSUMPTIONS

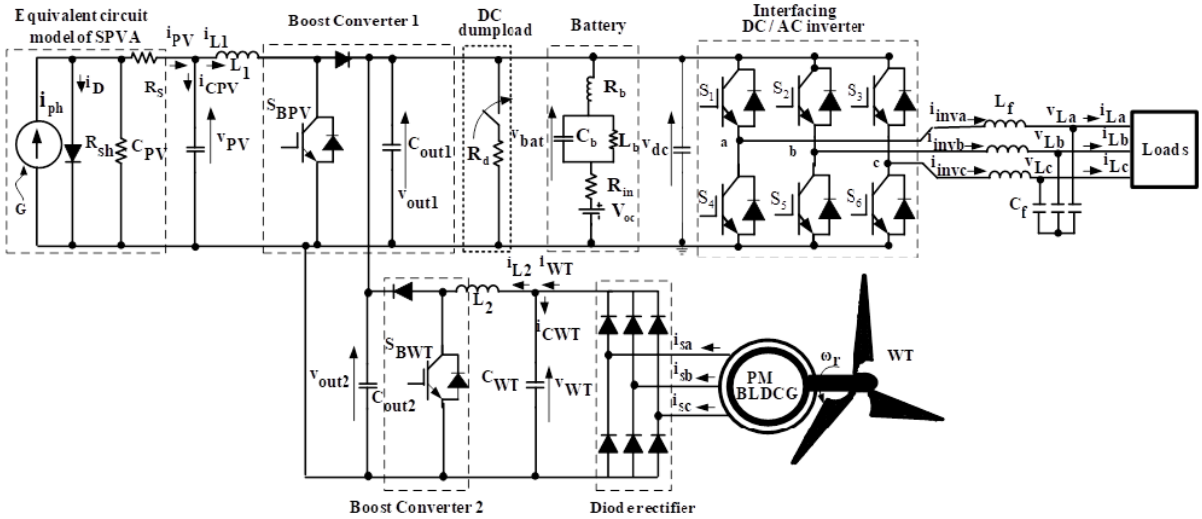

Fig. [1] Block diagram of the proposed system

The basic block diagram of the proposed HSPGS configuration is shown in fig (1). It consists of SPVA, two boost converters, Dc dump load, Battery, Wind turbine, Permanent magnet brushless DC generator, three-phase diode rectifier, DC-AC interfacing inverter, LC low pass filter and Load.

System Parameters

Elements	Parameters
SPVA Side	i_{rr}= 5.981*10^{-8} A, i_{scr}= 6A, K_i= 0.0024, T_r= 298K, q= 1.6*10^{-19} C, K_b= 1.38*10^{-23} J/K, E_g=1.12 V, A=1.2, C_{out1}=1000 µf, C_1=1000 µf, L_1=1.5 mH, K_1=50
WT Side	R_s=0.808, L_s= 5.44 mH, V_s= 208V, w_r= 1800rpm, L_{wt}= 1.5 mH, J=0.01859kg.cm^2, Km=80 V/tr/min, C_{out2}= 1000 µf, C_2= 1000 µf, 2P=4, K_2= 50
DC Bus	C_{dc}= 2500µf, V_{dc}=105 V, LA Batteries 9*(12V/12) Ah
AC Side	F_s= 60 Hz, V_{LL}= 50V, L_f= 5mH, C_f=40 µf linear load (R_L =8 ohm), nonlinear load (R_L=8 ohm, L_L= 20mH), K=3,

III.MODELING AND CONTROL STRATEGIES

Three control strategies are developed for the stable operation of HSPGS under sever conditions.

SPVA Modeling and Control design

The boost converter of SPVA, is modelled as follows.

$$L_1\left(\partial i_{L_1}/\partial t\right) = V_{PV} \quad (1)$$

$$C_{out1}\left(\partial V_{out_1}/\partial t\right) = -V_{out1}/R \quad (2)$$

$$i_{CPV} = C_{PV}\left(\partial V_{CPV}/\partial t\right) = i_{PV} - i_{L1} \quad (3)$$

When power switch is in off condition, i.e$S_{BPV} = 0$,

$$L_1\left(\partial i_{L_1}/\partial t\right) = V_{PV} - V_{out1} \quad (4)$$

$$C_{out1}\left(\partial V_{out_1}/\partial t\right) = i_{L1} - \left(V_{out1}/R\right) \quad (5)$$

| e-ISSN: 2278 – 8875, p-ISSN: 2320 – 3765| www.ijareeie.com | Impact Factor: 7.282|

|| Volume 10, Issue 8, August 2021 ||

| DOI:10.15662/IJAREEIE.2021.1008044 |

Where S_{BPV}-Switch, L_1-Inductance, C_{PV}-Input Capacitance, C_{out1}-Output Capacitance, R-Equivalent load resistance, i_{L1}-Inductor current, i_{PV}-Output PV current, i_{CPV}-Input capacitor current, V_{out1}-Output voltage, V_{CPV}-Input capacitor voltage. From above equations, the following equations for SPVA boost converter, are obtained as,

$$\left(\partial i_{L_1}/\partial t\right) = (V_{PV}/L_1 - (1 - d_1)(V_{out1}/L_1) \quad (6)$$

$$\left(\partial V_{out_1}/\partial t\right) = (1/C_{out1})[(i_{L1}(1 - d_1)) - (V_{out1}/R)] \quad (7)$$

Rearranging (6), we will get,

$$(\partial i_{PV}/\partial t) = (V_{PV}/L_1) - (1 - d_1)(V_{out1}/L_1) + C_{PV}(\partial^2 V_{PV}/\partial t^2) \quad (8)$$

Where d_1-Desired control.

The term, $C_{PV}(\partial^2 V_{PV}/\partial t^2)$ will be zero as there is no variation of V_{PV} during court duration. Hence, we can rewrite (8) as below,

$$(\partial i_{PV}/\partial t) = (V_{PV}/L_1) - (1 - d_1)(V_{out1}/L_1) \quad (9)$$

Control strategy for SPVA boost converter

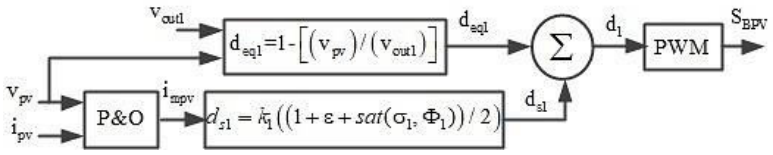

Fig. [2] Improved P&O based SMC with boundary layer for SPVA.

Sliding surface σ_1 is selected such that, system will reach surface and track MPP without loss of the control.

$$\sigma_1 = (\partial P_{PV}/\partial i_{PV}) = 0 \quad (10)$$

Where P_{PV}-Power generated from SPVA,

$$P_{PV} = V_{PV} i_{PV} \quad (11)$$

From (11), rewriting (10)

$$\sigma_1 = (\partial P_{PV}/\partial i_{PV}) = \partial(V_{PV} i_{PV})/\partial i_{PV} \quad (12)$$

From fig. [2] we can rearrange (12) as,

$$\sigma_1 = V_{PV} + i_{mPV}(\partial V_{PV}/\partial i_{mPV}) \quad (13)$$

Where i_{mPV}-Optimal PV current output obtained from classical P&O method, d_1- Structure of the chosen control, d_{s1}-Switching control, d_{eq1}- Equivalent control,

The chosen control and switching control are defined as below,

$$d_1 = d_{eq1} + d_{s1} \quad (14)$$

$$d_{s1} = K_1((1 + \varepsilon + \text{sat}(\sigma_1, \emptyset_1))/2 \quad (15)$$

With,

$$\text{sat}(\sigma_1, \emptyset_1)\begin{Bmatrix} 1 & \sigma_1 \succ \emptyset_1 \\ \sigma_1/\emptyset_1 & |\sigma_1| \leq \emptyset_1 \\ -1 & \sigma_1 \prec \emptyset_1 \end{Bmatrix} \quad (16)$$

K_1- Positive control gain, ε- Very small value, $\emptyset_1$- Sliding layer (0.5 to -0.5)

If derivative of sliding control σ_1 is set to be zero, then only we can obtain equivalent control.

| e-ISSN: 2278 – 8875, p-ISSN: 2320 – 3765| www.ijareeie.com | Impact Factor: 7.282|

|| Volume 10, Issue 8, August 2021 ||

| DOI:10.15662/IJAREEIE.2021.1008044 |

$\partial\sigma_1/\partial t = (\partial\sigma_1/\partial i_{mPV})(\partial i_{mPV}/\partial t)$

$\partial\sigma_1/\partial t = (\partial\sigma_1/\partial i_{mPV})[(V_{PV}/L_1) - (1-d_1)(V_{out1}/L_1)]$ (17)

The non-trivial solution is,

$V_{PV} - (1-d_1)V_{out1} = 0$ (18)

And the equivalent control is obtained as,

$d_{eq1} = 1 - [(V_{PV})/(V_{out1})]$ (19)

System stability analysis

$V_1 = (1/2)\sigma_1^2$ (20)

The system is globally stable if,

$(\partial V_1/\partial t) = \sigma_1(\partial\sigma_1/\partial t) < 0$ (21)

Putting (13) and (17) into (21),

$$V_{PV} + i_{mPV}(\partial V_{PV}/\partial i_{mPV})(2(\partial V_{PV}/\partial i_{mPV}) + i_{mPV}(\partial^2 V_{PV}/\partial^2 i_{mPV})) \quad (22)$$

$((V_{PV}/L_1) - (1-d_1)(V_{out1}/L_1)) < 0$

The system stability can be verified by the Lyapunov function candidate as,
Where output PV voltage,

$$V_{PV} = (K_b TA/q)\ln(i_{ph} + i_D - i_{L1})/i_D \quad (23)$$

Where K_b- Boltzmann's constant, T- Cell Temperature, A- Ideality factor, q- Charge of an electrons, i_{ph}-Light generated current, i_D- Saturation current, i_{L1}- Inductor current
First and second derivative of output PV voltage, are described as,

$$\partial V_{PV}/\partial i_{L1} = -(K_b TA/q)(i_D/(i_{ph} + i_D - i_{L1})) \quad (24)$$

$$\partial^2 V_{PV}/\partial^2 i_{L1} = -(K_b TA/q)(i_D/(i_{ph} + i_D - i_{L1})^2) \quad (25)$$

The sign of $V_{PV} + i_{mPV}(\partial V_{PV}/\partial i_{mPV})$ is always positive, and sign of $((V_{PV}/L_1) - (1-d_1)(V_{out1}/L_1))$ must be positive to verify the stability conditions.
From all the above equations the following condition must be valid for stable operation of the system.

$$(V_{out1}/L_1)\, K_1((1 + \varepsilon + \mathrm{sat}(\sigma_1, \emptyset_1))/2) > 0 \quad (26)$$

(V_{out1}/L_1) and $((1 + \varepsilon + \mathrm{sat}(\sigma_1, \emptyset_1))/2)$ are always positive hence to satisfy the stability condition as mentioned in (26) control gain K_1 must be positive.
WT Modeling and control design
The arrangements made in the system such that it is possible to achieve MPPT without measuring rotor position or wind speed.

Mathematical Model of PMBLDCG:

$$[V_{sabc}] = R_s[i_{sabc}] + (L_s - M)[di_{sabc}/dt] + [e_{abc}] \quad (27)$$

Where V_{sabc}- Terminal voltages, i_{sabc}- Terminal currents, R_s- Stator resistance, L_s-Stator inductor, M- Mutual inductor, e_{abc}- Back emf of PMBLDCG.

The electromagnetic torque of the PMBLDCG is,

$T_e = (1/\omega_r)(e_a i_{WTa} + e_b i_{WTb} + e_c i_{WTc})$ (28)

Where ω_r- Mechanical motor speed $\omega_r = (2/P)\omega_e$, ω_e- Electrical frequency, P- Number of rotor poles

| e-ISSN: 2278 – 8875, p-ISSN: 2320 – 3765| www.ijareeie.com | Impact Factor: 7.282|

|| Volume 10, Issue 8, August 2021 ||

| DOI:10.15662/IJAREEIE.2021.1008044 |

The motion of PMBLDCG is described as, $T_m = T_e + J(dw_r/d_t) + B\omega_r$ Where T_m- Developed torque, T_e- Electromagnetic torque, J- Moment of inertia, B- Friction coefficient.

Mathematical model of the WT boost converter:

For $S_{BWT} = 1$i.e. ON condition,

$$L_2(\partial i_{L2}/\partial t) = V_{WT} \quad (29)$$

$$C_{out2}(\partial V_{out2}/\partial t) = -V_{out2}/R \quad (30)$$

$$i_{CWT} = C_{WT}(\partial V_{CWT}/\partial t) = i_{WT} - i_{L2} \quad (31)$$

And for $S_{BWT} = 0$ i.e OFF condition

$$L_2(\partial i_{L2}/\partial t) = V_{WT} - V_{out2} \quad (32)$$

$$C_{out2}(\partial V_{out2}/\partial t) = i_{WT} - V_{out2}/R \quad (33)$$

Where S_{BWT},L_2, C_{WT}, C_{out2}, R, i_{L2}, i_{WT}, i_{CWT}, V_{CWT}, and V_{out2} represents switch,, inductance, input and output capacitances, equivalent load resistance, inductor current, output PV current, input capacitor current, input capacitor voltage, and output voltage of the WT side boost converter respectively.

From (29) to (33),

$$(\partial(i_{WT} - i_{CWT})/\partial t) = (\partial(i_{WT} - C_{WT}\partial V_{WT})/\partial t \quad (34)$$
$$= (V_{WT}/L_2) - (1 - d_2)(V_{out2}/L_2)$$

$$(\partial V_{out2}/\partial t) = (1/C_{out2})[i_{WT}(1 - d_2) - (V_{out2}/R) \quad (35)$$

Rearranging (34),

$$(\partial i_{WT}/\partial t) = (V_{WT}/L_2) - (1 - d_2)(V_{out2}/L_2) + C_{WT}(\partial^2 V_{WT}/\partial t^2) \quad (36)$$

Where, d_2 is the desired control for WT side boost converter.

The second derivative of V_{WT} is equal to zero. Hence, becomes

$$(\partial i_{WT}/\partial t) = (V_{WT}/L_2) - (1 - d_2)(V_{out2}/L_2) \quad (37)$$

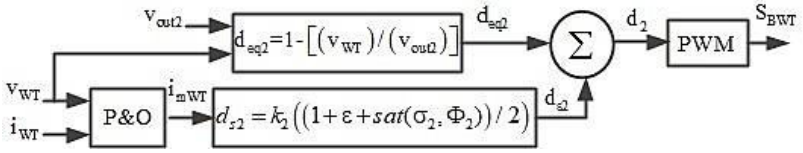

Fig. [3] Improved P&O based SMC with boundary layer for WT.

Sliding surface σ_2 is selected such that, system will reach surface and track MPP without loss of the control.

$$\sigma_2 = (\partial P_{dcWT}/\partial i_{WT}) = 0 \quad (38)$$

$$P_{dcWT} = V_{WT} i_{WT} \quad (39)$$

$$\sigma_2 = V_{WT} + i_{mWT}(\partial V_{WT}/\partial i_{mWT}) \quad (40)$$

Where $i_{WT}, P_{dcWT}, i_{mWT}$ represents Dc current, power generated from WT, and optimal current obtained using classical P&O method.

The chosen control and switching control are defined as below,

$$d_2 = d_{s2} + d_{eq2} \quad (41)$$

$$d_{s2} = K_2((1 + \varepsilon + sat(\sigma_2, \emptyset_2))/2) \quad (42)$$

| e-ISSN: 2278 – 8875, p-ISSN: 2320 – 3765| www.ijareeie.com | Impact Factor: 7.282|

|| Volume 10, Issue 8, August 2021 ||

| DOI:10.15662/IJAREEIE.2021.1008044 |

With,

$$sat(\sigma_{2,}\emptyset_2)\begin{Bmatrix} 1 & \sigma_2 \succ \emptyset_2 \\ \sigma_2/\emptyset_2 & |\sigma_2| \leq \emptyset_2 \\ -1 & \sigma_2 \prec \emptyset_2 \end{Bmatrix} \quad (43)$$

Where K_2, d_{eq2} and $\emptyset_2$, represents the control gain, equivalent control, and sliding layer (0.5 to -0.5)

If derivative of sliding control σ_1 is set to be zero, then only we can obtain equivalent control.

$$(\partial\sigma_2/\partial t) = (\partial\sigma_2/\partial i_{mWT})(\partial i_{mWT}/\partial t)$$

$$(\partial\sigma_2/\partial t) = (\partial\sigma_2/\partial i_{mWT})[(V_{WT}/L_2) - (1-d_2)(V_{out2}/L_2)] = 0 \quad (44)$$

The non-trivial solution is,

$$(V_{WT} - (1-d_2)V_{out2}) = 0 \quad (45)$$

And the equivalent control is obtained as,

$$d_{eq2} = 1 - [V_{WT}/V_{out2}] \quad (46)$$

System stability analysis

The system stability can be verified by the Lyapunov function candidate as,

$$V_2 = (1/2)\sigma_2^2 \quad (47)$$

The system is globally stable if,

$$(\partial V_2/\partial t) = \sigma_2(\partial\sigma_2/\partial t) < 0 \quad (48)$$

Putting (40) and(44) into (48),

$$(\partial V_2/\partial t) = (V_{WT} + i_{mWT}(\partial V_{WT}/\partial i_{mWT}))(2(\partial V_{WT}/\partial i_{mWT}) + \partial i_{mWT}(\partial^2 V_{WT}\partial^2 i_{mWT})) \quad (49)$$

$$((V_{WT}/L_2) - (1-d_2)(V_{out2}/L_2)) < 0$$

An output DC voltage, $V_{WT} = 2K_m\omega_r$Where K_m- motor back EMF constant, ω_r- rotor mechanical speed.

The rotor speed and output DC current are interrelated and expressed as,

$$\omega_r = 3.1i_{mWT} + 46 \quad (50)$$

Therefore $V_{WT} = K_m(6.2i_{mWT} + 92)$

For stability analysis the sign of $(V_{WT} + i_{mWT}(\partial V_{WT}/\partial i_{mWT}))(2(\partial V_{WT}/\partial i_{mWT}),\partial i_{mWT}(\partial^2 V_{WT}\partial^2 i_{mWT}))$and $((V_{WT}/L_2) - (1-d_2)(V_{out2}/L_2))$ is verified separately. The sign of first two terms are positive and therefore, the term $((V_{WT}/L_2) - (1-d_2)(V_{out2}/L_2))$ must be negative to satisfy stability condition.

Replacing (42),(46) in $((V_{WT}/L_2) - (1-d_2)(V_{out2}/L_2))$,

$$(V_{out2}/L_2)\,K_2((1 + \varepsilon + sat(\sigma_{2,}\emptyset_2))/2) < 0 \quad (51)$$

(V_{out2}/L_2) and $((1 + \varepsilon + sat(\sigma_{2,}\emptyset_2))/2)$ terms are always positive. Hence, to satisfy the stability condition, the control gain K_2 must be negative.

Three-phase inverter Modeling and control design

| e-ISSN: 2278 – 8875, p-ISSN: 2320 – 3765| www.ijareeie.com | Impact Factor: 7.282|

|| Volume 10, Issue 8, August 2021 ||

| DOI:10.15662/IJAREEIE.2021.1008044 |

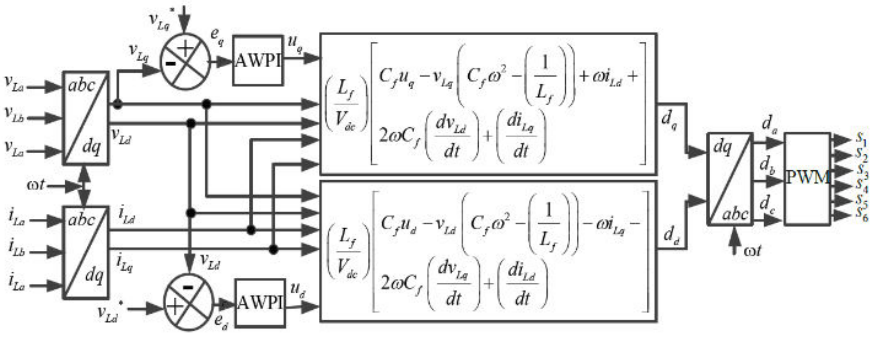

Fig. [4] APC based AWPI controller for three-phase interfacing inverter.

The following equations in natural three-phase (a-b-c) coordinated system, are obtained by applying Kirchhoff's voltage and current laws at the connection point.

$$(di_{inv(abc)}/dt) = (1/L_f)(d_{(abc)}V_{dc} - V_{L(abc)} \quad (52)$$

$$(dV_{L(abc)}/dt) = (1/C_f)(i_{inv(abc)} - i_{L(abc)}) \quad (53)$$

Where $d_{(abc)}, V_{Labc}, V_{dc}, i_{inv(abc)}, i_{L(abc)}, L_f$ and C_f represents the control variable, AC voltages, DC link voltage, output inverter currents, load currents, , inductance and capacitance of the inverter output filter, respectively.

To get the relations in d, q rotating axis, apply Park's transformation to (52) and (53).

$$(di_{invd}/dt) = (V_{dc}/L_f)d_d + i_{invq}\omega + V_{Ld} \quad (54)$$

$$(di_{invq}/dt) = (V_{dc}/L_f)d_q - i_{invd}\omega + V_{Lq}$$

$$(dV_{Ld}/dt) = (1/C_f)(i_{invd} - i_{Ld}) + \omega V_{Lq} \quad (55)$$

$$(dV_{Lq}/dt) = (1/C_f)(i_{invq} - i_{Lq}) - \omega V_{Ld}$$

After replacing (54) in the derivative of (55), we will get,

$$C_f(d^2V_{Lq}/dt^2) = V_{Lq}(C_f\omega^2 - (1/L_f)) - 2\omega C_f(dV_{Ld}/dt) + (V_{dc}/L_f)\, d_q - \omega i_{Ld} - (di_{Lq}/dt) \quad (56)$$

$$C_f(d^2V_{Ld}/dt^2) = V_{Ld}(C_f\omega^2 - (1/L_f)) + 2\omega C_f(dV_{Lq}/dt) + (V_{dc}/L_f)\, d_q + \omega i_{Lq} - (di_{Ld}/dt)$$

Where u_d, u_q – new equivalent inputs, pulsation $\omega = 2\pi f_s$, f_s – System frequency 60 Hz.

From (56) the control laws d_q and $d_d$are,

$$d_q = (L_f/V_{dc})[C_f u_q - V_{Lq}(C_f\omega^2 - (1/L_f)) + \omega i_{Ld} + 2\omega C_f(dV_{Ld}/dt) + (di_{Lq}/dt)] \quad (57)$$

$$d_d = (L_f/V_{dc})[C_f u_d - V_{Ld}(C_f\omega^2 - (1/L_f)) - \omega i_{Ld} - 2\omega C_f(dV_{Lq}/dt) + (di_{Ld}/dt)]$$

The tracking controllers $u_q$and u_d are obtained as follows,

$$u_q = (k\tau_c(\tau_i s + 1)/\tau_i(\tau_c s + 1))e_q + (1/(\tau_c s + 1))u_{qmax} \quad (58)$$

$$u_d = (k\tau_c(\tau_i s + 1)/\tau_i(\tau_c s + 1))e_d + (1/(\tau_c s + 1))u_{dmax}$$

Where $e_{d,q}$ is dq-axis AC voltage error, $V_{L\,d,q}$ is dq-axis AC voltage and k, τ_i, τ_c are Proportional, integral, feedback gain coefficients, respectively.

| e-ISSN: 2278 – 8875, p-ISSN: 2320 – 3765| www.ijareeie.com | Impact Factor: 7.282|

|| Volume 10, Issue 8, August 2021 ||

| DOI:10.15662/IJAREEIE.2021.1008044 |

IV.RESULT AND DISCUSSION

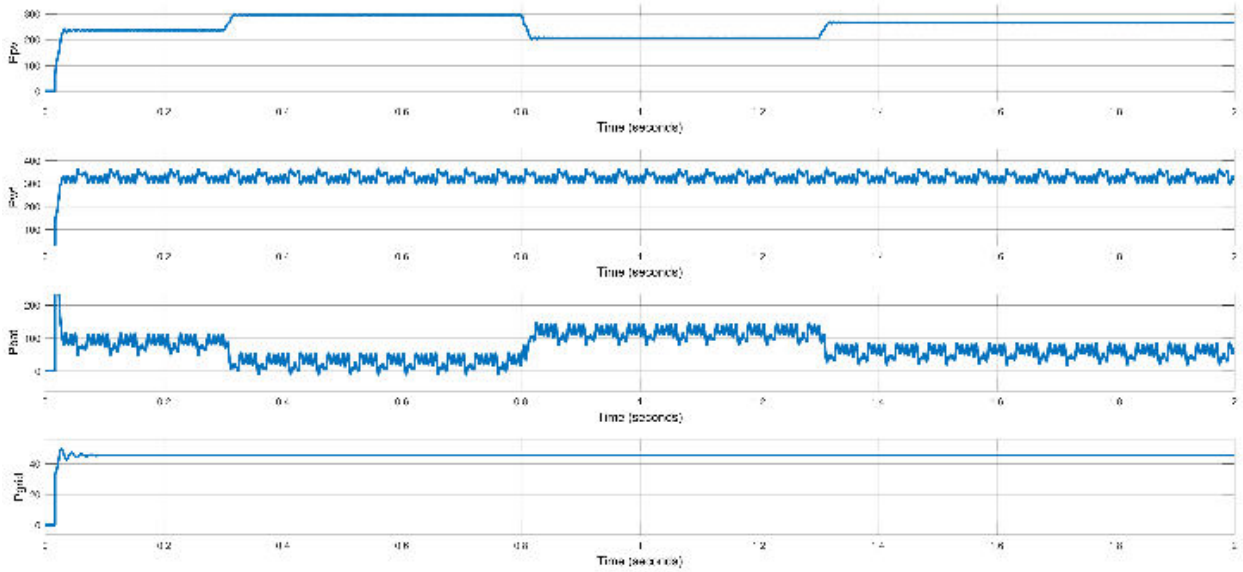

Fig. [5] (a)Ppv, (b)Pres, (c)Pbat, (d)Pgrid with conventional P&O method

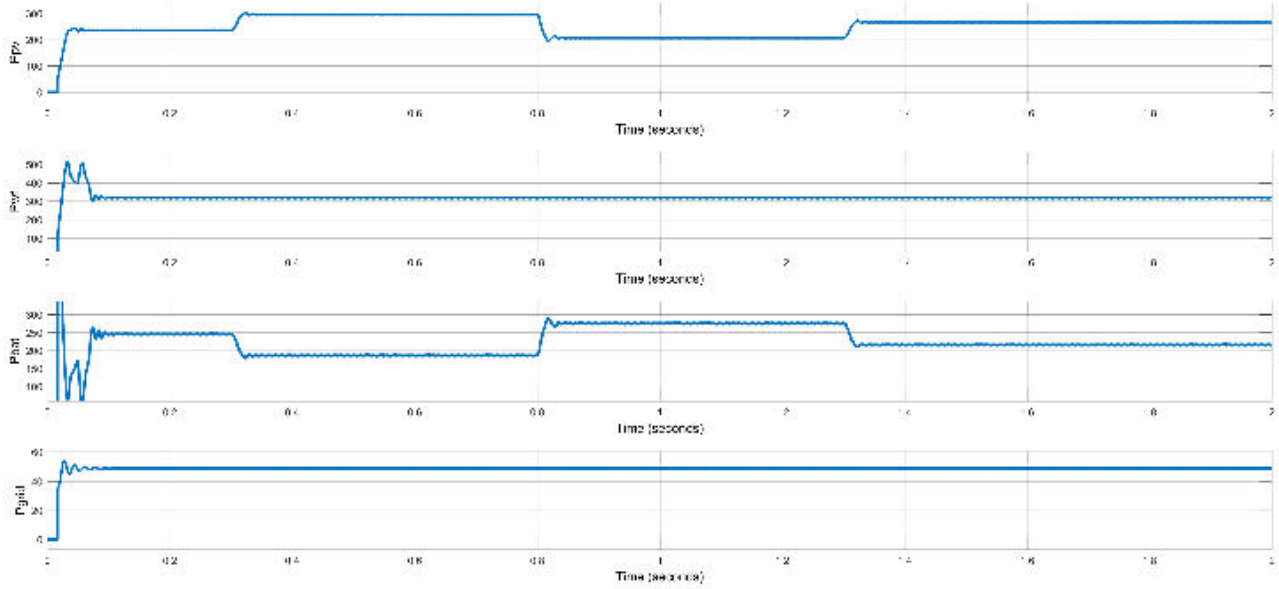

Fig. [6] (a)Ppv, (b)Pres, (c)Pbat, (d)Pgrid with Improved P&O, SMC method

| e-ISSN: 2278 – 8875, p-ISSN: 2320 – 3765| www.ijareeie.com | Impact Factor: 7.282|

|| Volume 10, Issue 8, August 2021 ||

| DOI:10.15662/IJAREEIE.2021.1008044 |

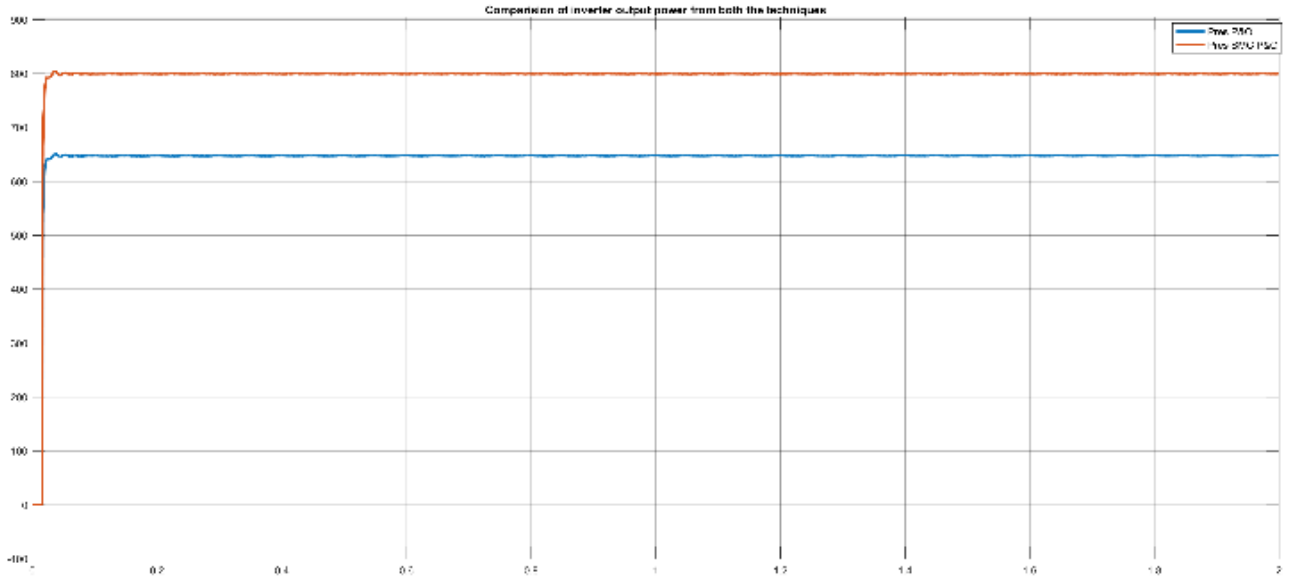

Fig. [7] Comparison of Pres with both techniques

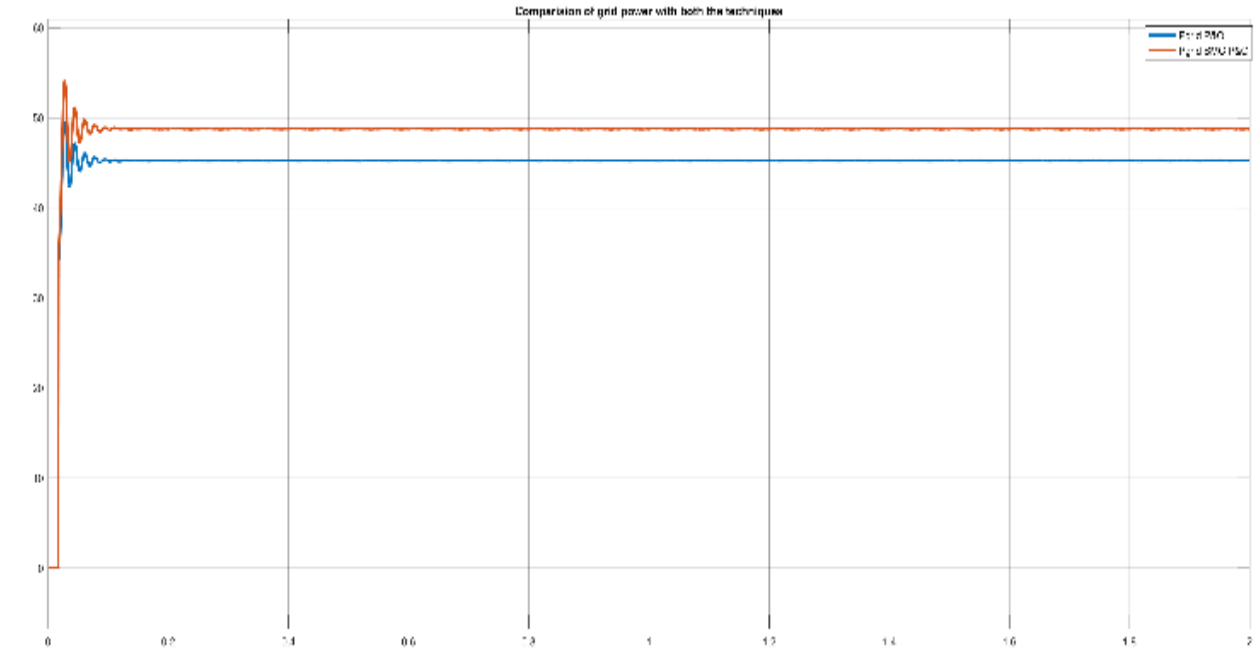

Fig. [8] Comparison of Pgrid with both techniques

The solar insolation input is increased, decreased, and increased again with respect to the finite time intervals at t=0.3, t=0.8, and t=1.3 seconds. It is observed that PV solar output current follows its reference during increase and decrease in solar insolation. MPPT from SPVA is achieved quickly without control divergence with conventional P&O technique and Improved P&O technique. However, desired control (d1) is not affected due to variation of solar insolation and simultaneously operation of WT side boost converter, and the three-phase interfacing inverter. The system is working within the defined range during transient and steady state conditions with improved P&O based SMC with boundary layer. This confirms the robustness of the improved P&O method over conventional P&O method. Fig. [5] shows the waveforms of the SPVA output power (Ppv), Battery power (Pbat), inverter output power (Pres) and Grid Power (Pgrid) for the system using conventional P&O method. Fig. [6] shows the waveforms of the SPVA output

| e-ISSN: 2278 – 8875, p-ISSN: 2320 – 3765| www.ijareeie.com | Impact Factor: 7.282|

|| Volume 10, Issue 8, August 2021 ||

| DOI:10.15662/IJAREEIE.2021.1008044 |

power (Ppv), Battery power (Pbat), inverter output power (Pres) and Grid Power (Pgrid) for the system using improved P&O method with SMC boundary level technique.

The comparative outputs in the form of Pres and Pgrid are shown in the fig. [7,8] These outputs are only for one condition for simplification, like these results the improved P&O method with SMC boundary level technique gives better outputs in transient and steady state condition as compared to conventional P&O method. The tests also performed for balanced and unbalanced nonlinear load, disconnected load condition. Because of the SMC AWPI controller system perform well during transient and steady state without any saturation and control divergence.

VI.CONCLUSION

The grid connected wind-PV-battery based hybrid power generation system has been proposed. Modeling, control design, and stability analysis have been presented in detail for both the techniques. Simulated performance of the system has been obtained with conventional P&O method and an improved P&O method for MPPT of SPVA and WT. For a multiple source hybrid power generation system, SMC with boundary layer is designed with P&O method for improved performance under variable weather conditions. It has been demonstrated that the improved P&O based MPPT is more reliable and efficient than conventional P&O method during weather changes in presence of many power converters operated simultaneously. The APC with AWPI voltage controller used in both the models, regulates constant and sinusoidal AC voltage without any saturation and overshoot during transients.

From all the results obtained one can conclude that, The Improved P&O with SMC boundary layer gives better outputs and stability of the system during transient and steady state condition than the conventional P&O method.

REFERENCES

[1] A.C. Luna, N.L.D. Aldana, M. Gracells, J.C. Vasquez, and J. M. Guerrero, “Mixed-Integer-Linear-Programming based Energy Management System for Hybrid PV-Wind-Battery Microgrids: Modeling, Design and Experimental Verification,” IEEE Trans. Power Electro. Vol. 32, no4, pp.2769-2783, April 2017.

[2] D. Li and Z.Q. Zhu, “A Novel Integrated Power Quality Controller for Microgrid,” IEEE Trans. Ind. Electr, vol. 62, no5, pp. 48-58. May 2015.

[3] M.A.G de Brito, L Galotto, L.P. Sampaio, G. de A. e Melo, and C.A. Canesin, “Evaluation of the Main MPPT Techniques for Photovoltaic Applications,” IEEE Trans. Industrial electronics, Vol. 60, No 3, pp.56-67, March 2013.

[4] TrishanEsram, P.L Chapman, “Comparison of Photovoltaic Array Maximum Power Point Tracking Techniques,” IEEE Trans. Industrial electronics.

[5] K.H. Kim, T.L. Van, D.C. Lee, S.H. Song, and E.H. Kim, “Maximum Output Power Tracking Control in Variable-Speed Wind Turbine Systems Considering Rotor Inertial Power,” IEEE Trans. Industrial electronics, vol.60, no8, pp. 3207-3217, Aug. 2013.

[6] J. Ahmed and Z. Salam, “A Modified P&O Maximum Power Point Tracking Method with Reduced Steady State Oscillation and Improved Tracking Efficiency,” IEEE Trans. Sus. Energy, vol. 7, no4, pp 1506-1515, Oct.2016.

[7] X. Li, H. Wen, L. Jiang, W. Xiao, Y. Du, and C. Zhao, “An Improved MPPT Method for PV system with Fast-Converging Speed and Zero Oscillation,” IEEE Trans. Ind. Applications, vol. 52, no 6, pp. 5051-5064, Dec. 2016.

[8] A. Pandey, N. Dasgupta, and A. K. Mukerjee, “High-Performance Algorithms for Drift Avoidance and Fast Tracking in Solar MPPT System,” IEEE Trans. Energy Conversion, vol. 23, no 2, pp. 681-689, June 2008.

[9] E. Mamarelis, G. Petrone, and G. Spagnuolo, “A Hybrid Digital-Analog Sliding Mode Controller for Photovoltaic Applications,” IEEE Trans. Ind. Informatics, vol. 9, no2, pp. 1094-1103, May 2013.

[10] Y. Levron and D. Shmilovitz, “Maximum Power Point Tracking Employing Sliding Mode Control,” IEEE Transactions on Circuits and Systems I: Regular Papers, vol. 60, no3, pp. 724-732, March 2013.

[11] B. Beltran, T. Ahmed-Ali, and M. E. H. Benbouzid, “Sliding Mode Power Control of Variable-Speed Wind Energy Conversion Systems,” IEEE Trans. Energy Conversion, vol. 23, no2, pp. 551-558, June 2008.

[12] J. W. Jung, N. T. T. Vu, D. Q. Dang, T. D. Do, Y. S. Choi, and H. H. Choi, “A Three-Phase Inverter for a Standalone Distributed Generation System: Adaptive Voltage Control Design and Stability Analysis,” IEEE Trans. Energy Conversion, vol. 29, no1, pp. 46-56, March, 2014.

[13] D. Q. Dang, Y. S. Choi, H. H. Choi, and J. W. Jung, “Experimental Validation of a Fuzzy Adaptive Voltage Controller for Three-Phase PWM Inverter of a Standalone DG Unit,” IEEE Trans. Ind. Informatics, vol. 11, no3, pp. 632-641, June 2015.

[14] Z. Wang, W. Wu, and B. Zhang, “A Distributed Quasi-Newton Method for Droop-Free Primary Frequency Control in Autonomous Microgrids,” IEEE Trans. Smart Grid, vol. PP, pp. 1-1, 2016.

| e-ISSN: 2278 – 8875, p-ISSN: 2320 – 3765| www.ijareeie.com | Impact Factor: 7.282|

|| Volume 10, Issue 8, August 2021 ||

| DOI:10.15662/IJAREEIE.2021.1008044 |

[15] Q. C. Zhong, "Robust Droop Controller for Accurate Proportional Load Sharing Among Inverters Operated in Parallel," IEEE Trans. Ind. Electro., vol. 60, no 4, pp. 1281-1290, April 2013.

[16] X. Tang, X. Hu, N. Li, W. Deng, and G. Zhang, "A Novel Frequency and Voltage Control Method for Islanded Microgrid Based on Multienergy Storages," IEEE Trans. Smart Grid, vol. 7, no1, pp. 410-419, Jan. 2016.

[17] H. Shi, F. Zhuo, H. Yi, F. Wang, D. Zhang, and Z. Geng, "A Novel Real-Time Voltage and Frequency Compensation Strategy for Photovoltaic-Based Microgrid," IEEE Trans. Ind. Electro, vol. 62, no6, pp. 3545-3556, June 2015.

[18] W. Wang, Y. Li, Y. Cao, U. Haeger, and C. Rehtanz, "Adaptive Droop Control of MTDC System for Frequency Support and Power Sharing," IEEE Trans. Power Systems, vol. Early access, pp. 1-1, 2017.

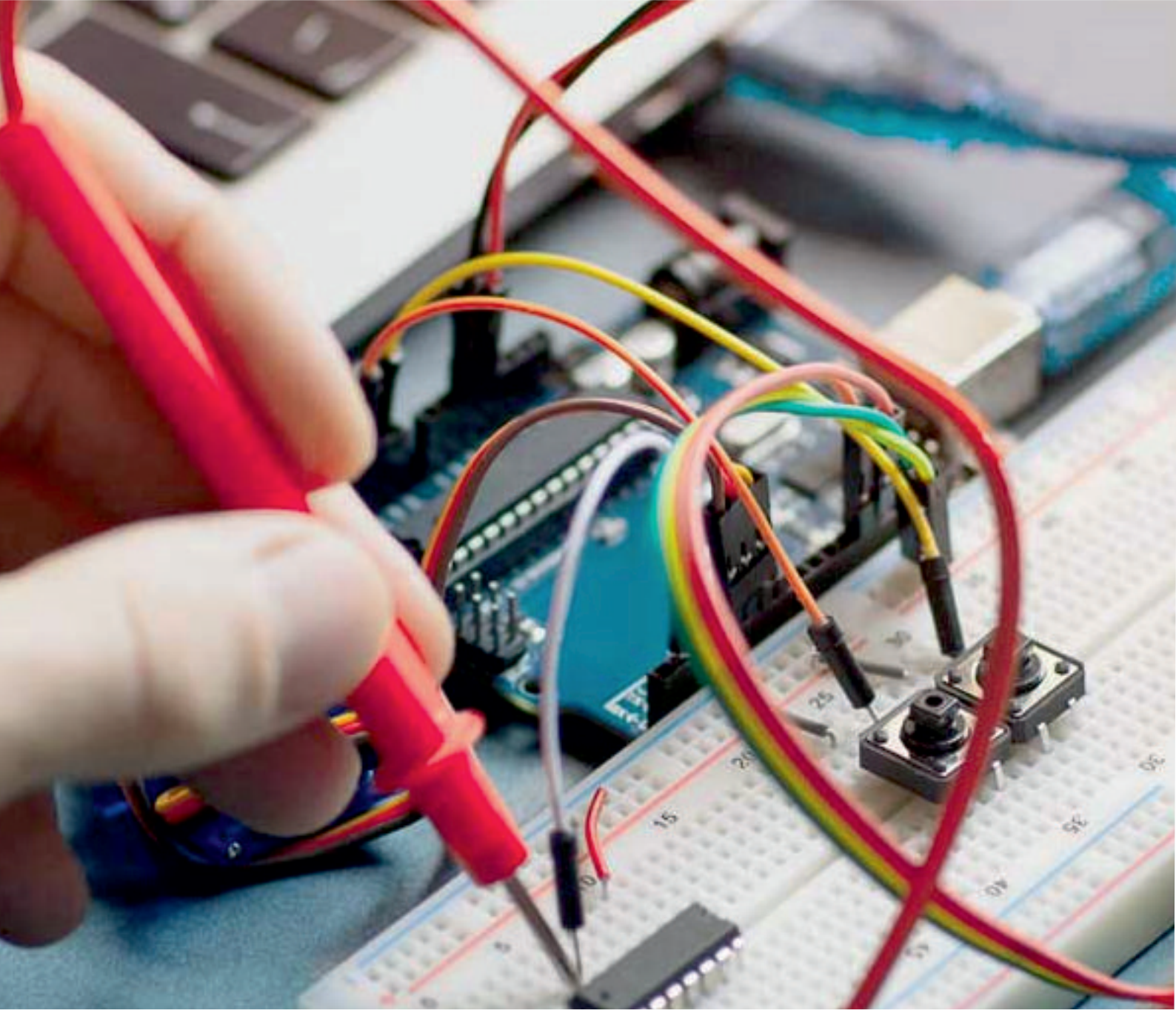

INNO SPACE
SJIF Scientific Journal Impact Factor

Impact Factor: 7.282

doi cross ref

ISSN INTERNATIONAL STANDARD SERIAL NUMBER INDIA

निस्केयर NISCAIR

International Journal of Advanced Research

in Electrical, Electronics and Instrumentation Engineering

9940 572 462 6381 907 438 ijareeie@gmail.com

www.ijareeie.com

Scan to save the contact details